Available online at www.sciencedirect.com
SCIENCE DIRECT®
Journal of Sound and Vibration 290 (2006) 1100–1118
JOURNAL OF SOUND AND VIBRATION
www.elsevier.com/locate/jsvi

Free vibration analysis of skewed open circular cylindrical shells

Selvakumar Kandasamy, Anand V. Singh*

Department of Mechanical and Materials Engineering, The University of Western Ontario, London, Ont., Canada N6A 5B9

Received 3 November 2004; received in revised form 29 March 2005; accepted 7 May 2005
Available online 8 August 2005

Abstract

In this paper, a numerical study is presented for the free vibration of skewed open circular cylindrical deep shells. The formulation considers first-order shear deformation theory of shells and includes rotary inertia and shear deformation so that thin-to-moderately thick shells can be analyzed. A set of grid points, the number of which depends upon the orders of the polynomials chosen for the displacement and rotation components, on the middle surface of the shell is defined first. For a particular displacement component, the field functions are derived corresponding to each node from the above-mentioned set of points and are used in the Rayleigh–Ritz method to calculate frequencies and mode shapes. Convergence study with reference to the order of the polynomials used for the displacement fields was performed first. Numerical results obtained from the present method are compared with those from the finite element method and very good agreement is observed. Additional results are presented and discussed in this paper for skewed panels clamped at the curved edges and free at the straight parallel edges.

1. Introduction

In the published monograph (NASA SP – 288) by Leissa [1], one can find that the shell vibrations research has been reported as early as 1888 by Lord Rayleigh and A.E.H. Love. This research topic has since attracted many researchers and many review articles have appeared in the

*Corresponding author. Tel.: +1 519 661 2111x88321; fax: +1 519 661 3020.
E-mail address: avsingh@eng.uwo.ca (A.V. Singh).

0022-460X/$ - see front matter © 2005 Elsevier Ltd. All rights reserved.
doi:10.1016/j.jsv.2005.05.010

Nomenclature

E	modulus of elasticity
h	thickness of the shell
k	shear correction factor
$[K]$	stiffness matrix
L	length
$[M]$	mass matrix
R	radius of the middle surface
u, v, w	displacement components in x, θ, z directions
x, θ, z	coordinates in axial, circumferential and radial directions
v	Poisson's ratio
Ω	$\omega R\sqrt{\rho/E}$, dimensionless frequency parameter
ω	circular frequency in radian/second
ρ	mass density of the shell material
β_1, β_2	parameters associated with the rotation of the normal to the middle surface
θ_0	subtended angle of the cylindrical panel
ξ, η	natural coordinates

literature. Recently published work by Qatu [2,3] has mentioned papers published during the period 1989–2000 on the dynamic behavior of homogeneous and composite shells with main thrust on the free vibration. In the reference section, Qatu has also included review articles by others after 1973. Owing to the applications of open shell structures in aerospace, automotive, civil, marine and mechanical engineering, open rectangular cylindrical shallow and deep panels have been studied quite extensively. Results corresponding to both the shallow and deep rectangular shell panels are available in the literature. Works on the vibrations of shallow cylindrical shells on triangular, trapezoidal and rhombic planforms have also been reported in the literature and are not mentioned in the present study as their citations are already available in recently published review papers by many. Only selective published works are mentioned briefly in the present study.

Selmane and Lakis [4] presented dynamic and static analysis of thin open cylindrical shells freely supported along their curved edges and the straight edges are subjected to different boundary conditions. Bardell et al. [5] analyzed the free vibration problem for completely free deep cylindrical panel using h–p version of the finite element method (FEM) and then the method was extended to study thin isotropic conical panels [6]. They used cubic Hermite polynomials as the element shape functions and enriched the displacement field by orthogonal polynomials. Using Rayleigh–Ritz method and parametric Bezier functions in the admissible displacement fields, Singh [7] studied the free vibration of deep doubly curved sandwich shell panels. In this paper, he compared numerical results from the Rayleigh–Ritz method with those from I-DEAS for isotropic circular cylindrical and spherical shell panels. Rectangular-type open circular cylindrical composite shell supported on various combinations of corner and mid-edge points of the panel was investigated by Singh and Shen [8]. It appears from the authors experience that there are not many publications on the free vibration of open skewed circular cylindrical deep panels in the literature.

The present study deals with the free vibration analysis of isotropic skewed open circular cylindrical shells using modified version of the Rayleigh–Ritz method. The method follows the FEM, but only one subparametric element is used in the analysis. In the initial steps, the elasticity equations are defined in the cylindrical coordinate system. The form of the equations is reduced from 3D to 2D using the middle surface of the cylindrical shell as the reference. Then, the natural

coordinates are used to define the geometry by prescribing the axial and circumferential coordinates at the four corner points of the skewed panel and four bilinear shape functions are used for this purpose. To generate the displacement fields, a different set of grid points are selected on the reference surface of the shells. A few of the displacement nodes may coincide with those used for the geometry. The number of the displacement grid points depends solely on the orders of the polynomials used in each of the two natural coordinates and is considerably higher than the number of geometric points. By working in the natural coordinate system, expressions for the stiffness and mass matrices are derived. To assess the applicability of the method, the convergence study is first carried out for thin and moderately thick cylindrical panels using 45° skew angle and subtended angles of 30°, 45° and 60°. The panel is assumed to be clamped at the two parallel curved edges and the straight parallel edges in the longitudinal direction are kept free. Next, the results from the present method are compared with the same from a commercial FE code I-DEAS. After satisfactory resolutions, further results are presented in the graphical form showing the variation of the first five frequencies with the thickness-to-radius ratio for subtended angles 30–75° at the interval of 15°. Different length-to-radius ratios starting from 0.50 to 4.00 have been used in the present study.

2. Formulation

Open circular cylindrical shells have been studied by many great researchers of the time of 1930–1960 [9]. Using the force–moment–balance method or the energy method, the differential equations of equilibrium (or motion) were derived in terms of stress and moment resultants. Then the equations were simplified using the Hooke's law and the strain–displacement relations to obtain the final form prior to the solution phase in terms of the displacement components. Also, plate and shell problems were solved by many [9] using the "*stress function*", which was introduced by G.B. Airy in 1862 to solve 2D elasticity problems [10]. The elasticity problems dealing with continuous systems were also solved by considering both the displacement and stress function as the primary unknown variables and the method was called the "*mixed method*". The many practical problems were solved in closed form during this period. In the late fifties of the last century, scientists and engineers started solving problems using numerical methods on digital computers and displacement-based FEM came into existence. This computationally efficient method grew very rapidly in its first 20 years, became increasingly popular and many commercial codes were developed during that period, because of it was based on the solid foundation of the minimization of the potential energy. FEM also followed the same trend as the classical methods in the fields of stress analysis, vibration and buckling of continuous systems by having purely displacement based, mixed and hybrid formulations. Because of the digital computers, the century old Rayleigh–Ritz method began attracting the attention of the researchers in the field of vibration of beams, plates and shells and consequently many papers have appeared in the literature after 1970.

The method developed in this paper is a modified form of the Rayleigh–Ritz method to investigate the free vibration analysis of open circular cylindrical shells. Fig. 1 shows the middle surface of an isotropic open shell having thickness h, length L, radius R, mass density ρ and subtended angle θ_0. This middle surface of the shell is considered as the reference surface along

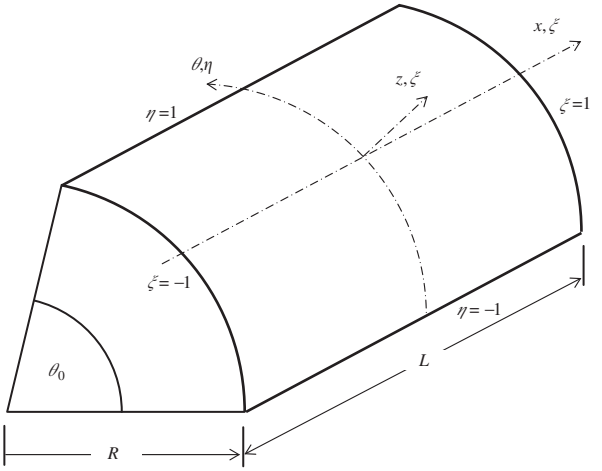

Fig. 1. Middle surface of the circular cylindrical panel with dimensions and coordinate system.

which the axial (x), circumferential (θ) and radial (z) coordinate system is defined. Three displacement components u', v' and w' are also defined at an arbitrary location x, θ, and z, respectively. These are further expressed in terms of u, v, w, β_1 and β_2 as shown below for a circular cylindrical shell.

$$u'(\theta, x, z) = u(\theta, x) + \zeta\beta_1(\theta, x),$$

$$v'(\theta, x, z) = v(\theta, x)(1 + \zeta) + \zeta\beta_2(\theta, x),$$

$$w'(\theta, x, z) = w(\theta, x). \tag{1}$$

Here u, v and w denote the displacement components in the axial (x), circumferential (θ), and radial (z) directions, respectively. Symbols β_1 and β_2 correspond to the components of the rotation of the normal to the middle surface of the shell in axial and circumferential directions, respectively, and are made to have the same unit as displacement components using the radius R. The thickness coordinate z is normalized using the radius R of the middle surface of the shell by introducing a parameter $\zeta = z/R$, which is assumed to be $\zeta \ll 1.0$ for thin-to-moderately thick shell. Also, one should note that $(1 + \zeta)$, which appear with $v(x, \theta)$ in Eq. (1) due to the curvature in the circumferential direction, is absent from the first of the above three equations. This is because of the reason that the curvature is zero along the x-axis. In vector/matrix form, Eq. (1) appears as

$$\{\Delta'\} = \begin{bmatrix} 1 & 0 & 0 & \zeta & 0 \\ 0 & 1+\zeta & 0 & 0 & \zeta \\ 0 & 0 & 1 & 0 & 0 \end{bmatrix} \begin{Bmatrix} u \\ v \\ w \\ \beta_1 \\ \beta_2 \end{Bmatrix} = [\Gamma]\{\Delta\}. \tag{2}$$

The strain–displacement relations for the cylindrical shell are derived from the elasticity equations [11] and are presented in the following form:

$$\varepsilon'_{xx} = \frac{\partial u'}{\partial x}, \quad \varepsilon'_{\theta\theta} = \frac{1}{R}\left(\frac{1}{1+\zeta}\right)\left(\frac{\partial v'}{\partial \theta} + w'\right),$$

$$\varepsilon'_{\theta x} = \frac{1}{R}\left(\frac{1}{1+\zeta}\right)\frac{\partial u'}{\partial \theta} + \frac{\partial v'}{\partial x}, \quad \varepsilon'_{xz} = \frac{\partial u'}{\partial z} + \frac{\partial w'}{\partial x},$$

$$\varepsilon'_{\theta z} = \frac{\partial v'}{\partial z} + \frac{1}{R}\left(\frac{1}{1+\zeta}\right)\left(\frac{\partial w'}{\partial \theta} - v'\right). \tag{3}$$

By using Eq. (1) and approximating $(1+\zeta)^{-1} \approx (1-\zeta)$, one can reduce Eq. (3) to the following matrix form:

$$\{\varepsilon'\}_{5\times 1} = [\gamma]_{5\times 15}\{\chi\}_{15\times 1}, \tag{4}$$

where $\{\varepsilon'\} = \{\varepsilon'_{xx}\ \varepsilon'_{\theta\theta}\ \varepsilon'_{\theta x}\ \varepsilon'_{xz}\ \varepsilon'_{\theta z}\}$, $\{\chi\}^{\mathrm{T}} = \{\chi_1\ \chi_2\ \chi_3\ \cdots\ \chi_{14}\ \chi_{15}\}$ and

$$[\gamma] = \begin{bmatrix} 1 & \zeta & \zeta^2 & 0 & 0 & 0 & 0 & 0 & 0 & 0 & 0 & 0 & 0 & 0 & 0 \\ 0 & 0 & 0 & 1 & \zeta & \zeta^2 & 0 & 0 & 0 & 0 & 0 & 0 & 0 & 0 & 0 \\ 0 & 0 & 0 & 0 & 0 & 0 & 1 & \zeta & \zeta^2 & 0 & 0 & 0 & 0 & 0 & 0 \\ 0 & 0 & 0 & 0 & 0 & 0 & 0 & 0 & 0 & 1 & \zeta & \zeta^2 & 0 & 0 & 0 \\ 0 & 0 & 0 & 0 & 0 & 0 & 0 & 0 & 0 & 0 & 0 & 0 & 1 & \zeta & \zeta^2 \end{bmatrix}. \tag{5}$$

Eq. (4) also has been arranged in the same manner as Eq. (2) where the thickness parameter(ζ) is separated from other parameters that correspond to the reference surface of the shell. Matrix $[\gamma]$ is composed of the thickness parameter only, whereas the components of vector $\{\chi\}$ in Eq. (4) are formed with strain and curvature like terms at the middle surface of the shell and are given below.

$$\chi_1 = \frac{\partial u}{\partial x}, \quad \chi_2 = \frac{\partial \beta_1}{\partial x}, \quad \chi_3 = 0,$$

$$\chi_4 = \frac{1}{R}\left(\frac{\partial v}{\partial \theta} + w\right), \quad \chi_5 = -\frac{w}{R} + \frac{1}{R}\frac{\partial \beta_2}{\partial \theta},$$

$$\chi_6 = -\frac{1}{R}\frac{\partial \beta_2}{\partial \theta},$$

$$\chi_7 = \frac{1}{R}\frac{\partial u}{\partial \theta} + \frac{\partial v}{\partial x}, \quad \chi_8 = \frac{\partial v}{\partial x} - \frac{1}{R}\frac{\partial u}{\partial \theta} + \frac{\partial \beta_2}{\partial x} + \frac{1}{R}\frac{\partial \beta_1}{\partial \theta},$$

$$\chi_9 = -\frac{1}{R}\frac{\partial \beta_1}{\partial \theta}, \quad \chi_{10} = \frac{\partial w}{\partial x} + \frac{\beta_1}{R},$$

$$\chi_{11} = \chi_{12} = 0, \quad \chi_{13} = \frac{1}{R}\frac{\partial w}{\partial \theta} + \frac{\beta_2}{R}, \quad \chi_{14} = -\chi_{13}, \quad \chi_{15} = \frac{\beta_2}{R}. \tag{6}$$

The stress–strain relationship can be written as

$$\{\sigma'\} = [E']\{\varepsilon'\}, \tag{7}$$

where $\{\sigma'\}^{\mathrm{T}} = \{\sigma'_{xx}\ \sigma'_{\theta\theta}\ \tau'_{\theta x}\ \tau'_{xz}\ \tau'_{\theta z}\}$ and $[E']$ is a fifth-order elasticity matrix, which can be used to define both isotropic and anisotropic material properties. But for the present analysis, the material is assumed to be isotropic and the non-zero components of $[E']$ matrix are given by

$$E'_{11} = E'_{22} = \frac{E}{1-\nu^2}, \quad E'_{12} = E'_{21} = \frac{\nu E}{1-\nu^2}, \quad E'_{33} = \frac{E}{2(1+\nu)}, \quad E'_{44} = E'_{55} = kE'_{33}, \tag{8}$$

where ν is the Poisson's ratio and E is the Young's modulus of the shell material. The above matrix equations are derived by applying the concept of thin shell theory to the general 3D elasticity equations in cylindrical coordinates. The preceding equations are valid for both the closed and open circular cylindrical shells.

With the assumed distribution of u' and v' in Eq. (1) along the thickness will produce nearly constant shear strain and hence shear stress also linear along the thickness of the shell. This is in contrast to the parabolic distribution of transverse shear stress in bending of plates and shells, where the shear stresses are supposed to be zero at the inside and outside surfaces and maximum at the middle surface of the shell. To incorporate the parabolic distribution in an overall sense in the analysis of thin-to-moderately thick plates and shells, researchers have used a shear correction factor, which has also been considered in this paper by introducing k in Eq. (8). The commonly used value of this shear correction factor is either $(\pi^2/12)$ as proposed by Mindlin [12] or (5/6) by Reissner as discussed by Mindlin in his paper [12]. The value of (5/6) for the shear correction factor was also suggested by Naghdi [13] who proposed thin shell theory including rotary inertia and transverse shear deformation terms. Since this factor has a very minor role in the overall response of thin plates and shells and both values are very close, either one can be used to obtain basically the same values of the natural frequencies.

It can be seen in Fig. 2(a) that a rectangular panel similar to the one shown in Fig. 1 can be obtained by cutting the 3D surface by a set of two planes that are perpendicular to the x-axis and separated by length L. Similarly, a skewed cylindrical panel can be obtained by rotating the same set of cutting planes by an angle α in the clockwise direction. In the top view, Fig. 2(b), the projected surface of the skewed panel is shown along with the cutting planes mentioned above. The reference surface is defined by prescribing x and θ coordinates of the four corner points (x_j, θ_j) for $j = 1, 2, 3, 4$. The $(x-\theta)$ coordinates of an arbitrary point on the reference surface of the shell can be interpolated by using the natural coordinate system (ξ, η) in the following manner [14].

$$\theta(\xi,\eta) = \sum_{j=1}^{4} N_j(\xi,\eta)\theta_j \quad \text{and} \quad x(\xi,\eta) = \sum_{j=1}^{4} N_j(\xi,\eta)x_j. \tag{9}$$

In the above, $N_j(\xi, \eta)$ is known as the "*shape function*". The next step in the process is to define the displacement fields in terms of ξ and η coordinates for each of u, v, w, β_1 and β_2. To achieve this, a different set of grid points, which are different from the geometric nodes on the reference surface, is considered. These points are given separate identities, are termed as the displacement nodes, and may fall on the four corner points coinciding with the geometric nodes. By referring to the earlier work of Singh and Muhammad [15], it is seen that the grid size of the displacement nodes depends upon the orders of interpolating polynomials in ξ and η. The form of the displacement

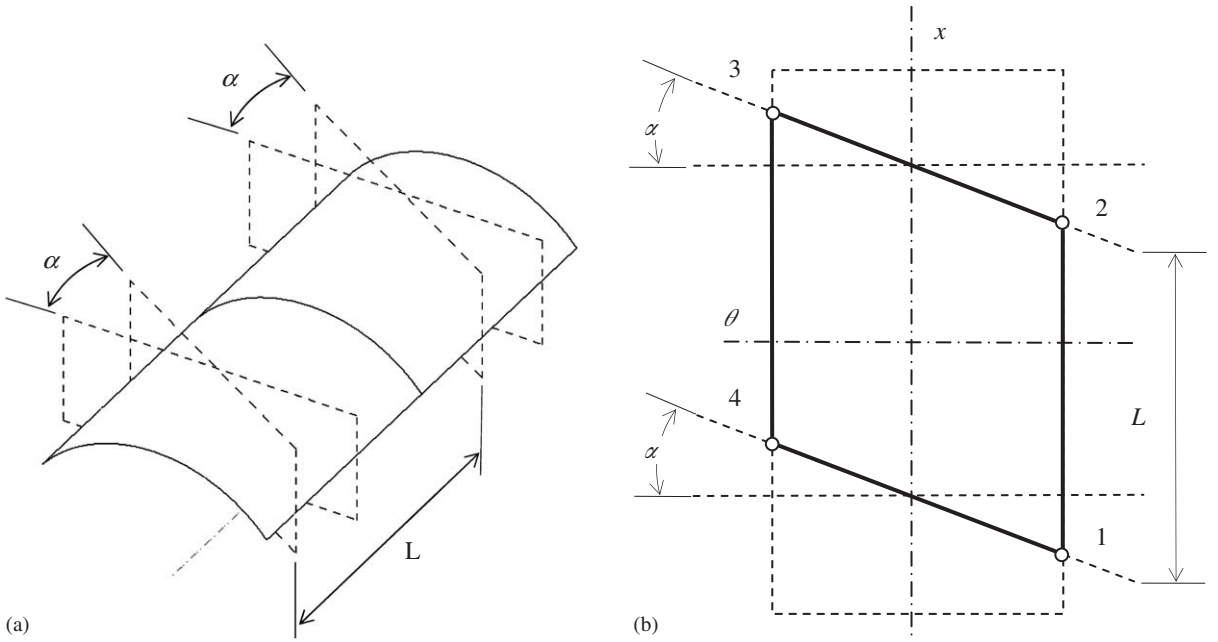

Fig. 2. 3D and top views of the cylindrical panel with intersecting planes.

field is same as that for the coordinates as given in Eq. (9), except that these are created with relatively high-order interpolating functions and are given as follows.

$$u = \sum_{j=1}^{p} u_j N_j(\xi,\eta), \quad v = \sum_{j=1}^{p} v_j N_j(\xi,\eta), \quad w = \sum_{j=1}^{p} w_j N_j(\xi,\eta),$$

$$\beta_1 = \sum_{j=1}^{p} \beta_{1j} N_j(\xi,\eta), \quad \beta_2 = \sum_{j=1}^{p} \beta_{2j} N_j(\xi,\eta), \tag{10}$$

where $p = (p_1 + 1) \times (p_2 + 1)$, $p_1 =$ order of the polynomial in ξ, similarly $p_2 =$ order of the polynomial in η, and $N_j(\xi,\eta)$ corresponds to the *jth displacement shape function* and will be different from the ones used for the geometry, Eq. (9), but the procedure to obtain these is the same for both cases. Now, substituting Eq. (10) for $u, v, w, \beta_1,$ and β_2 into Eq. (6), the χ vector can be expressed as

$$\{\chi\} = [B]\{q\}, \tag{11}$$

where the B-matrix contains *shape functions* $N_i(\xi,\eta)$ and their derivatives with respect to ξ and η. Due to large size of $[B]$, i.e. $15 \times P$, where $P = 5 \times p$, it is not included in this paper. The vector $\{q\}^{\mathrm{T}} = \{u_i\ v_i\ w_i\ \beta_{1i}\ \beta_{2i}\}$ for $i = 1, 2, \ldots, p$ is made of the five dof of each displacement node. The strain energy expression can be written as

$$U = \frac{1}{2}\int_x \int_\theta \int_z \{\varepsilon'\}^{\mathrm{T}}\{\sigma'\}\, \mathrm{d}V.$$

Here the infinitesimal volume can further be written as

$$\mathrm{d}V = \mathrm{d}z(R+z)\,\mathrm{d}\theta\,\mathrm{d}x = R^2\mathrm{d}\zeta(1+\zeta)\,\mathrm{d}\theta\,\mathrm{d}x = R^2(1+\zeta)\,\mathrm{d}\zeta|J(\xi,\eta)|\,\mathrm{d}\xi\,\mathrm{d}\eta,$$

where $\mathrm{d}\theta\,\mathrm{d}x = |J(\xi,\eta)|\,\mathrm{d}\xi\,\mathrm{d}\eta$ and $|J(\xi,\eta)|$ = determinant of the Jacobian matrix [14]. By working on this energy expression with the help of Eqs. (7) and (11) and integrating over the thickness of the shell, the following matrix equation can be obtained:

$$U = \tfrac{1}{2}\{q\}^{\mathrm{T}}[K]_{P\times P}\{q\}, \tag{12}$$

where the stiffness matrix $[K]$ is given by,

$$[K]_{P\times P} = \frac{EL\theta_0}{4}\int_{-1}^{+1}\int_{-1}^{+1}[B]^{\mathrm{T}}[D][B]|J(\xi,\eta)|\,\mathrm{d}\xi\,\mathrm{d}\eta. \tag{13}$$

In the above, the 15th-order matrix $[D]$ is obtained due to integration over the thickness and is composed of geometric and material parameters of the panel.

The kinetic energy T of an isotropic cylindrical shell for the given displacement distribution can be calculated by

$$T = \frac{1}{2}\int_V \rho\left\{\left(\frac{\partial u'}{\partial t}\right)^2 + \left(\frac{\partial v'}{\partial t}\right)^2 + \left(\frac{\partial w'}{\partial t}\right)^2\right\}\mathrm{d}V = \frac{1}{2}\int_V \rho\left\{\frac{\partial \Delta'}{\partial t}\right\}^{\mathrm{T}}\left\{\frac{\partial \Delta'}{\partial t}\right\}\mathrm{d}V \tag{14}$$

where ρ is the density, V is the volume of the shell, and u', v' and w' are the displacement components along θ, x and z directions, respectively, as defined by Eq. (1). By using Eqs. (2) and (10) and integrating over the thickness of the shell, the following expression is obtained:

$$T = \tfrac{1}{2}\{\dot{q}\}^{\mathrm{T}}[M]_{P\times P}\{\dot{q}\}$$

where over-dot represents the time derivative of the spatial coordinates and $[M]$ is called the mass matrix as given by

$$[M]_{P\times P} = \frac{\rho R^2 L\theta_0}{4}\int_{-1}^{+1}\int_{-1}^{+1}[A]^{\mathrm{T}}[A_0][A]|J(\xi,\eta)|\,\mathrm{d}\eta\,\mathrm{d}\xi, \tag{15}$$

where $[A_0]$ = a fifth-order matrix resulting from the integration of $[\Gamma]^{\mathrm{T}}_{5\times 3}[\Gamma]_{3\times 5}$ over the thickness and $[A]$ =a $5\times P$ matrix consisting of the shape functions $N_j(\xi,\eta)$. Terms, attached to u, v and w, of matrix $[A_0]$ introduce translational inertia into the vibrating continuous system. Similarly, terms, attached with β_1 and β_2, adds rotary inertia, which has nearly negligible influence on the lower modes of vibration of thin plates and shells, but become quite significant at higher modes [12,16] and others). For moderately thick plates and shells, it is significant even at lower end of the frequency spectrum.

The exact integration over the thickness in Eqs. (13) and (15) is performed, whereas the Gauss method is used for the integration over the surface. An in-house object-oriented program in C++ has been developed incorporating the method presented briefly in the preceding section. The geometric parameters such as (L/R), (h/R), θ_0 representing length, thickness and subtended angle are chosen so that the numerical results have a wide range of applications. The frequency parameter is also made dimensionless by writing $\Omega = \sqrt{\rho/E}\omega R$. The numerical analysis is performed in this work on open skewed circular cylindrical panels clamped at the two curved edges and free at the remaining two straight edges and the value of the Poisson's ratio $v = 0.3$ has

been used throughout the work. First, the convergence study is carried out to examine the numerical stability of the method. Then, the procedure and results are validated through comparison of the results from the present method with those obtained from a commercial FE code I-DEAS. Some new results involving different geometric configurations and boundary conditions are also presented in the following sections.

3. Convergence study

Panel with the skew angle1 $\alpha = 45^\circ$ is chosen with the fixed curved edge and free straight edge conditions. The length-to-radius ratio $L/R = 0.5$ represents very short shell and thin-to-moderately thick shells are covered using $h/R = 0.01$ and 0.05, respectively. The shallow shell theory has been used by many researchers for the analysis of open cylindrical shells with subtended angle of up to $\theta_0 = 30^\circ$. Hence, subtended angles of $\theta_0 = 30^\circ$, 45° and 60° are considered in this paper to cover both the shallow and deep panels. The example with $\theta_0 = 60^\circ$ is a good representative case for deep open shell. Taking these parameters into consideration, natural frequencies of the first five modes are calculated and presented in Tables 1 and 2 for $h/R = 0.01$ and 0.05, respectively. The same order is used for polynomials in each of ξ and η and is shown by p_1 in column two of the tables. The matrix size dealt with in the calculation is $5(p_1 + 1)^2$ and the computation is performed using double precision. The frequency calculations for the convergence begins with $p_1 = 4$ and stops at $p_1 = 12$. Tables 1 and 2 show that the results are converging at a steady pace in all the cases. Convergence study was also performed by one of the authors of this paper [17] for the case with $\alpha = 0^\circ$ representing rectangular circular cylindrical panel and identical convergence characteristics have been reported there. To observe the convergence graphically, frequency parameter (Ω) is plotted against the order of the polynomial (p_1) and shown in Fig. 3 for the case with $\theta_0 = 60^\circ$ from Table 2. The levelling of the curves is clearly seen in this figure for the order of the polynomial 7 and higher. Hereafter, numerical results for various geometrical and/or physical parameters are obtained using $p_1 = p_2 = 12$ in the displacement fields given in Eq. (10). This translates into solving eigenvalue problem with the matrix order of $5(p_1 + 1)^2 = 845$.

4. Comparison with the finite element method

In order to validate the present method, frequencies for the first five modes are calculated by taking the subtended angles $\theta_0 = 30^\circ$ and 60° to represent, respectively, the shallow and deep shells and length-to-radius ratio $L/R = 0.5$ corresponding to a very short shell. The values of the thickness parameter chosen include $h/R = 0.05$, 0.01 and 0.005, which cover the range from moderately thick to very thin shells. Similarly, to examine the effects of the skew angle of the panel on the natural frequencies, calculations are performed with $\alpha = 0^\circ, 15^\circ, 30^\circ$ and 45°, wherein $\alpha = 0^\circ$ represents a rectangular circular cylindrical shell. Then the results are compared with those obtained from a commercial FE code I-DEAS. The FE mesh that was constructed for the analysis used 300 eight-node-shell-elements, 30 in the circumferential direction and 10 in the longitudinal direction. With this number of elements, the mesh consisted of 981 nodes, where as only 169

Table 1
Convergence of the non-dimensional frequency parameter $\Omega = \omega R\sqrt{\rho/E}$ for a skewed open cylindrical shell fixed at the curved edges

θ_0	p_1	Mode 1	Mode 2	Mode 3	Mode 4	Mode 5
30°	4	0.675	0.702	1.033	1.634	3.163
	5	0.577	0.580	0.954	1.078	1.512
	6	0.526	0.527	0.934	0.989	1.241
	7	0.515	0.517	0.922	0.957	1.123
	8	0.511	0.511	0.918	0.952	1.101
	9	0.508	0.508	0.916	0.950	1.097
	10	0.506	0.507	0.914	0.949	1.095
	11	0.506	0.506	0.914	0.948	1.093
	12	0.505	0.505	0.913	0.947	1.092
45°	4	0.708	0.718	1.018	1.161	1.946
	5	0.608	0.608	0.976	1.003	1.334
	6	0.545	0.549	0.953	0.982	1.026
	7	0.526	0.532	0.938	0.961	1.011
	8	0.518	0.519	0.932	0.949	1.008
	9	0.512	0.513	0.927	0.943	1.007
	10	0.510	0.509	0.925	0.940	1.007
	11	0.510	0.509	0.925	0.940	1.007
	12	0.506	0.507	0.923	0.937	1.007
60°	4	0.727	0.741	1.035	1.050	1.545
	5	0.640	0.649	0.987	1.027	1.137
	6	0.575	0.581	0.975	0.976	1.022
	7	0.544	0.550	0.957	0.960	1.021
	8	0.528	0.534	0.945	0.952	1.005
	9	0.521	0.521	0.940	0.942	0.996
	10	0.514	0.515	0.935	0.937	0.995
	11	0.511	0.511	0.932	0.934	0.995
	12	0.509	0.509	0.930	0.932	0.995

Parameters: $\alpha = 45°$, $h/R = 0.01$, $L/R = 0.5$, and order of the polynomial $p_1 = p_2$.

displacement nodes were used in the model from the present formulation. Results from the two methods are presented in Table 3. The comparison is seen to be extremely favorable, i.e. within one percent difference, except for the case with $\alpha = 45°$ where the difference appears to be in the neighborhood of three percent at higher modes. The values of the frequencies produced by the FE method in this case are consistently seen to be lower than those from the present method. From the experience of the authors of this paper, it seems that eight node isoparametric shell elements are inherently softer than its four-node counterparts. To have a graphical view of the comparison, results from Table 3 for the cases with $h/R = 0.01$ are plotted and shown in Figs. 4(a) for the 30° and Fig. 4(b) for the 60° subtended angles. Solid line represents curve for the rectangular panel and the skewed panels are represented by various types of broken lines. More comparison with the FE method is carried out for longer panels and results are presented in Table 4 for cases with

Table 2
Convergence of the non-dimensional frequency parameter $\Omega = \omega R\sqrt{\rho/E}$ for skewed open cylindrical shell fixed at the curved edges

θ_0	p_1	Mode 1	Mode 2	Mode 3	Mode 4	Mode 5
30°	4	2.242	2.315	3.129	5.130	5.399
	5	2.112	2.114	2.857	3.807	5.038
	6	2.044	2.045	2.790	3.591	4.622
	7	2.021	2.029	2.779	3.516	4.415
	8	2.018	2.022	2.775	3.510	4.364
	9	2.013	2.019	2.774	3.507	4.356
	10	2.012	2.017	2.773	3.506	4.351
	11	2.012	2.016	2.772	3.505	4.350
	12	2.006	2.014	2.772	3.505	4.349
45°	4	2.337	2.348	2.822	3.914	5.261
	5	2.148	2.171	2.666	3.001	4.671
	6	2.075	2.075	2.640	2.914	3.534
	7	2.048	2.046	2.636	2.887	3.431
	8	2.031	2.033	2.634	2.883	3.359
	9	2.024	2.025	2.633	2.880	3.354
	10	2.021	2.020	2.632	2.879	3.351
	11	2.018	2.018	2.632	2.878	3.350
	12	2.017	2.016	2.632	2.877	3.349
60°	4	2.379	2.410	2.714	3.331	4.879
	5	2.203	2.224	2.621	2.772	3.937
	6	2.102	2.122	2.607	2.728	3.013
	7	2.073	2.072	2.605	2.716	2.977
	8	2.051	2.049	2.604	2.713	2.939
	9	2.035	2.036	2.603	2.711	2.936
	10	2.027	2.028	2.603	2.710	2.934
	11	2.023	2.023	2.603	2.709	2.933
	12	2.020	2.020	2.602	2.708	2.932

Parameters: $\alpha = 45°$, $h/R = 0.05$, $L/R = 0.5$, and order of the polynomial $p_1 = p_2$.

$\alpha = 0°$ representing rectangular type and $\alpha = 45°$ the skewed type, respectively, for the same thickness-to-radius parameter of 0.01. Excellent agreement is seen also for the long cylindrical panels.

5. Frequency variation against the shell thickness

In this section, frequencies for open cylindrical shells having $L/R = 0.5$ and clamped on the curved edges are investigated against the thickness-to-radius ratio (h/R) of the shell. Skew angles $\alpha = 0°$ and 45° are considered along with subtended angles $\theta_0 = 30°$, 45°, 60° and 75° to cover the shallow-to-deep shells. Results with $\alpha = 0°$, which represents rectangular curved panel, are presented in Fig. 5 for the above four opening angles. As expected, value of the dimensionless frequency parameter Ω increases with the thickness parameter (h/R). In all cases, the frequencies

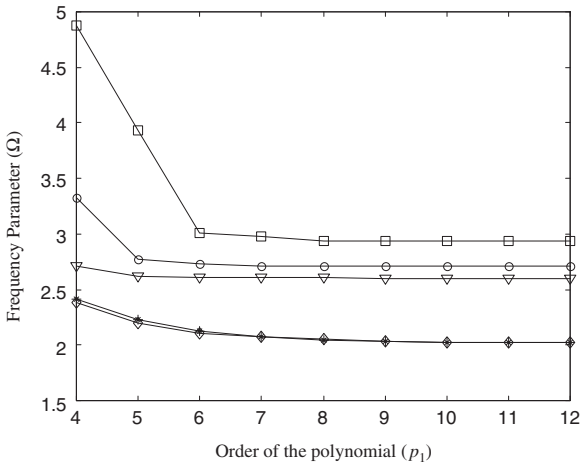

Fig. 3. Convergence of the non-dimensional frequency parameter $\Omega = \omega R\sqrt{\rho/E}$ for a skewed open cylindrical shell fixed at the curved edges with skew angle $\alpha = 45^\circ$, subtended angle $\theta_0 = 60^\circ$, $h/R = 0.05$ and $L/R = 0.5$.

of the first two modes are very close to each other and get even closer as the subtended angle increases. It is to be noted that for the case with $\theta_0 = 30^\circ$ and 45° frequencies are widely separated when $0.01 \leqslant h/R \leqslant 0.05$, whereas the frequency band gets narrow for deep shells with $\theta_0 = 60^\circ$ and 75°. Also, the values of the frequencies decrease as the subtended angle increases. Results for the set with $\alpha = 45^\circ$ are presented in Fig. 6, wherein the variation pattern of the frequencies for the skewed shell is observed to be very similar to that for the rectangular shells, but the values are slightly higher for the case of the skewed type. For the deep skew shells with $\theta_0 = 60^\circ$ and 75°, it is found that the frequencies for the first two natural modes are almost equal and the remaining three higher modes appear in clustered form. Plots of frequency parameter versus thickness to radius ratio have been generated as well with $L/R = 1.0$, but the results are not included in this paper, as the general trend for this case have been found to be very similar to frequency distribution of the shell with $L/R = 0.50$.

The above results have been obtained with the rotary inertia terms included in the formulation. However, the rotary inertia terms can be conveniently dropped from equations within the present setup by setting zero values to the last two rows and columns of matrix $[A_0]$ in Eq. (15). With this condition, a sample calculation was performed for the case presented in Table 2 with $\theta_0 = 30^\circ$ without the rotary inertia terms and the results obtained are: 2.023, 2.033, 2.808, 3.581, and 4.455 for the first five modes with $p_1 = 12$. The corresponding results from Table 2 including the rotary inertia are: 2.006, 2.014, 2.772, 3.505, and 4.345. As expected, lower values of the frequencies are found when the rotary inertia terms are included and the difference between the results from the two sets increases with the mode number.

6. Mode shapes

Mode shapes corresponding to the first five natural modes of the free vibration of both the rectangular ($\alpha = 0^\circ$) and skewed ($\alpha = 45^\circ$) shells are plotted and shown in Figs. 7 and 8,

Table 3
Comparison of the non-dimensional frequency parameter $\Omega = \omega R\sqrt{\rho/E}$ for a skewed open cylindrical shell fixed at the curved edges

θ_0	Mode	P-type	I-DEAS	P-type	I-DEAS	P-type	I-DEAS	P-type	I-DEAS
		$\alpha = 0^\circ$		$\alpha = 15^\circ$		$\alpha = 30^\circ$		$\alpha = 45^\circ$	
$h/R = 0.05$									
30°	1	1.314	1.307	1.375	1.366	1.585	1.567	2.006	1.979
	2	1.462	1.452	1.500	1.489	1.643	1.626	2.014	1.981
	3	2.269	2.272	2.271	2.274	2.340	2.338	2.772	2.746
	4	3.300	3.278	3.423	3.396	3.498	3.512	3.505	3.503
	5	3.511	3.488	3.626	3.599	3.929	3.893	4.349	4.332
60°	1	1.365	1.356	1.423	1.405	1.616	1.565	2.020	1.901
	2	1.383	1.375	1.435	1.419	1.614	1.563	2.020	1.901
	3	1.609	1.601	1.678	1.667	1.935	1.912	2.602	2.538
	4	1.924	1.915	1.960	1.948	2.133	2.107	2.708	2.625
	5	2.521	2.518	2.507	2.504	2.544	2.531	2.932	2.864
$h/R = 0.01$									
30°	1	0.359	0.358	0.374	0.373	0.421	0.419	0.505	0.500
	2	0.409	0.409	0.413	0.413	0.434	0.433	0.505	0.500
	3	0.627	0.626	0.651	0.650	0.736	0.734	0.913	0.909
	4	0.873	0.872	0.863	0.862	0.857	0.856	0.947	0.942
	5	0.900	0.899	0.903	0.901	0.980	0.976	1.092	1.086
60°	1	0.380	0.379	0.392	0.389	0.428	0.419	0.509	0.484
	2	0.382	0.381	0.393	0.390	0.428	0.419	0.509	0.484
	3	0.632	0.630	0.659	0.656	0.751	0.742	0.930	0.900
	4	0.633	0.632	0.661	0.659	0.762	0.752	0.932	0.902
	5	0.784	0.781	0.784	0.782	0.824	0.819	0.995	0.983
$h/R = 0.005$									
30°	1	0.227	0.227	0.234	0.234	0.255	0.254	0.295	0.292
	2	0.236	0.236	0.241	0.240	0.257	0.256	0.295	0.292
	3	0.487	0.487	0.486	0.485	0.512	0.510	0.591	0.587
	4	0.511	0.510	0.504	0.504	0.533	0.531	0.597	0.593
	5	0.511	0.511	0.534	0.533	0.582	0.579	0.687	0.682
60°	1	0.232	0.231	0.238	0.236	0.257	0.252	0.298	0.284
	2	0.233	0.232	0.238	0.236	0.257	0.252	0.298	0.284
	3	0.438	0.437	0.458	0.456	0.520	0.513	0.602	0.576
	4	0.446	0.445	0.463	0.461	0.528	0.520	0.602	0.576
	5	0.512	0.509	0.511	0.508	0.533	0.525	0.688	0.658

Parameter: $L/R = 0.5$, representing a short panel.

respectively. Both the 3D deformed surface and the contour plot on the developed surface are presented. By examining each mode one at a time, the first mode shown in Fig. 7(a) is symmetrical about both axes for the rectangular panel. The second mode shown in Fig. 7(b) is symmetric

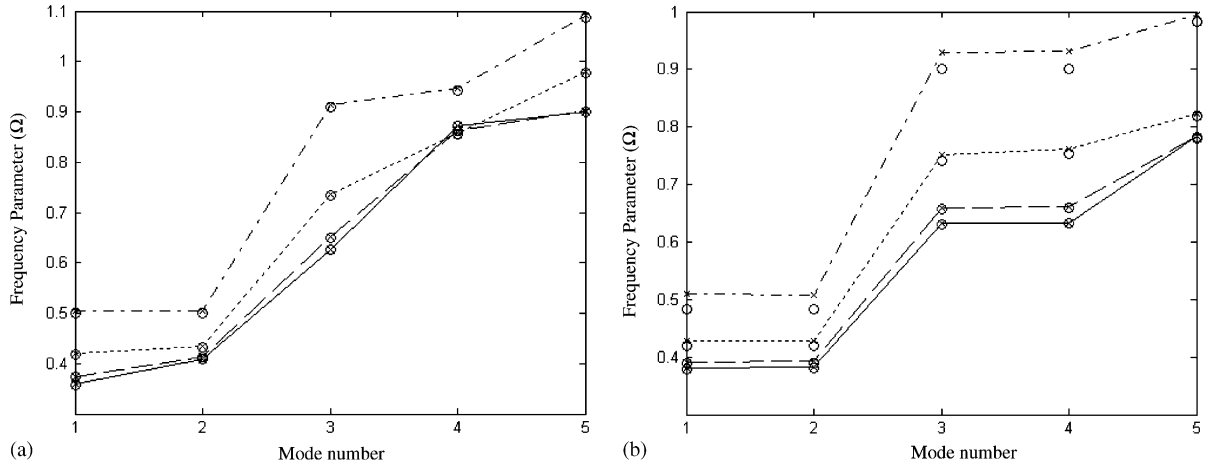

Fig. 4. Comparison of the non-dimensional frequency parameter $\Omega = \omega R\sqrt{\rho/E}$ for skewed open cylindrical shell fixed at the curved edges with $h/R = 0.01$, and $L/R = 0.5$: x-mark, p-type method; circle, I-DEAS; solid, skew angle $\alpha = 0^\circ$; dashed, $\alpha = 15^\circ$; dotted, $\alpha = 30^\circ$; dash-dot, $\alpha = 45^\circ$. (a) Subtended angle $\theta_0 = 30^\circ$ and (b) $\theta_0 = 60^\circ$.

Table 4
Comparison of the non-dimensional frequency parameter $\Omega = \omega R\sqrt{\rho/E}$ for open cylindrical shells fixed at the curved edges with $h/R = 0.01$

θ_0	Mode	P-type	I-DEAS	P-type	I-DEAS	P-type	I-DEAS	P-type	I-DEAS
		$L/R = 1.0$		$L/R = 2.0$		$L/R = 3.0$		$L/R = 4.0$	
$\alpha = 0^\circ$									
30°	1	0.120	0.120	0.046	0.046	0.025	0.025	0.014	0.014
	2	0.169	0.169	0.054	0.054	0.028	0.028	0.020	0.020
	3	0.281	0.280	0.101	0.100	0.059	0.059	0.039	0.039
	4	0.330	0.327	0.132	0.132	0.066	0.066	0.042	0.042
	5	0.338	0.337	0.167	0.167	0.095	0.094	0.066	0.065
60°	1	0.142	0.141	0.061	0.061	0.032	0.031	0.019	0.019
	2	0.153	0.151	0.069	0.068	0.054	0.054	0.043	0.043
	3	0.305	0.300	0.119	0.118	0.075	0.074	0.047	0.047
	4	0.305	0.303	0.129	0.128	0.078	0.077	0.063	0.063
	5	0.308	0.303	0.187	0.185	0.106	0.106	0.075	0.075
$\alpha = 45^\circ$									
30°	1	0.170	0.169	0.056	0.055	0.030	0.029	0.016	0.016
	2	0.188	0.187	0.066	0.066	0.032	0.031	0.022	0.022
	3	0.334	0.332	0.122	0.121	0.067	0.066	0.042	0.042
	4	0.368	0.366	0.133	0.133	0.072	0.071	0.046	0.045
	5	0.419	0.414	0.204	0.203	0.109	0.108	0.072	0.071
60°	1	0.181	0.177	0.074	0.073	0.040	0.039	0.024	0.023
	2	0.181	0.178	0.076	0.076	0.053	0.053	0.040	0.040
	3	0.349	0.341	0.130	0.129	0.080	0.079	0.059	0.058
	4	0.349	0.343	0.139	0.138	0.083	0.083	0.062	0.062
	5	0.449	0.435	0.208	0.206	0.120	0.120	0.084	0.083

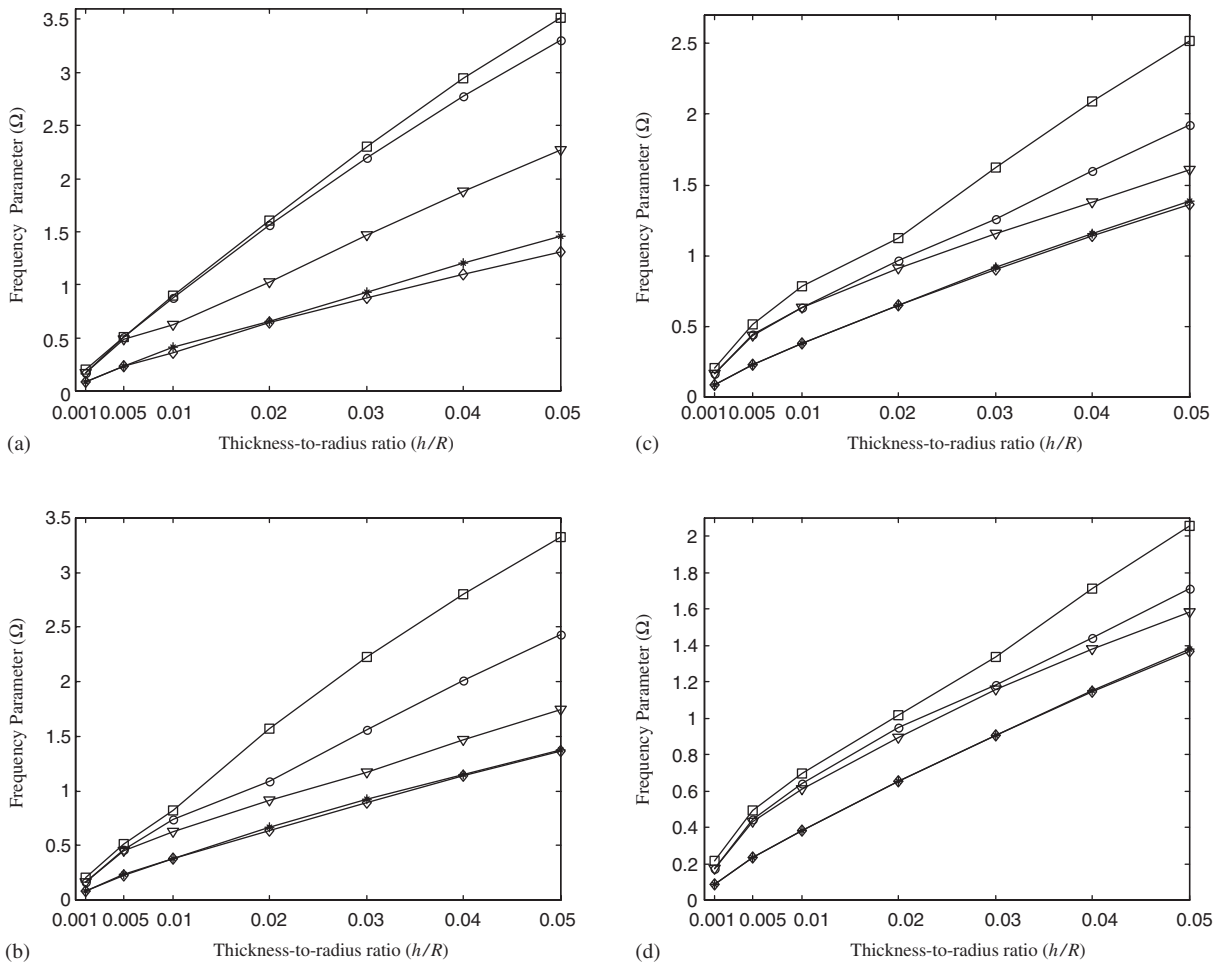

Fig. 5. Frequency parameter (Ω) versus thickness-to-radius ratio (h/R) for shells with skew angle $\alpha = 0^\circ$ and $L/R = 0.5$: diamond, mode 1; star, mode 2; triangle, mode 3; circle, mode 4; square, mode 5. (a) Subtended angle $\theta_0 = 30^\circ$; (b) $\theta_0 = 45^\circ$; (c) $\theta_0 = 60^\circ$ and (d) $\theta_0 = 75^\circ$.

about the circumferential axis and antisymmetric about the longitudinal axis. For the third mode, the symmetry and antisymmetry are opposite of the second mode. The behavior of the fourth mode is the same as that of the second mode, i.e. symmetric about the circumferential axis and antisymmetric about the longitudinal axis. The fifth mode is antisymmetric in both directions. For the rectangular open cylindrical panel, the symmetry and antisymmetry exist in both the wave form and the amplitude of vibration. One should note here that in classical method of solution of this problem, each mode shape is identified by the axial and circumferential mode numbers m and n, respectively, because the displacement fields are assumed in terms of transcendental functions with specified wavenumbers, e.g. $\sin mx$, $\cos n\theta$, etc. In the present numerical method, polynomials are considered in the displacement fields without any reference to the axial and circumferential

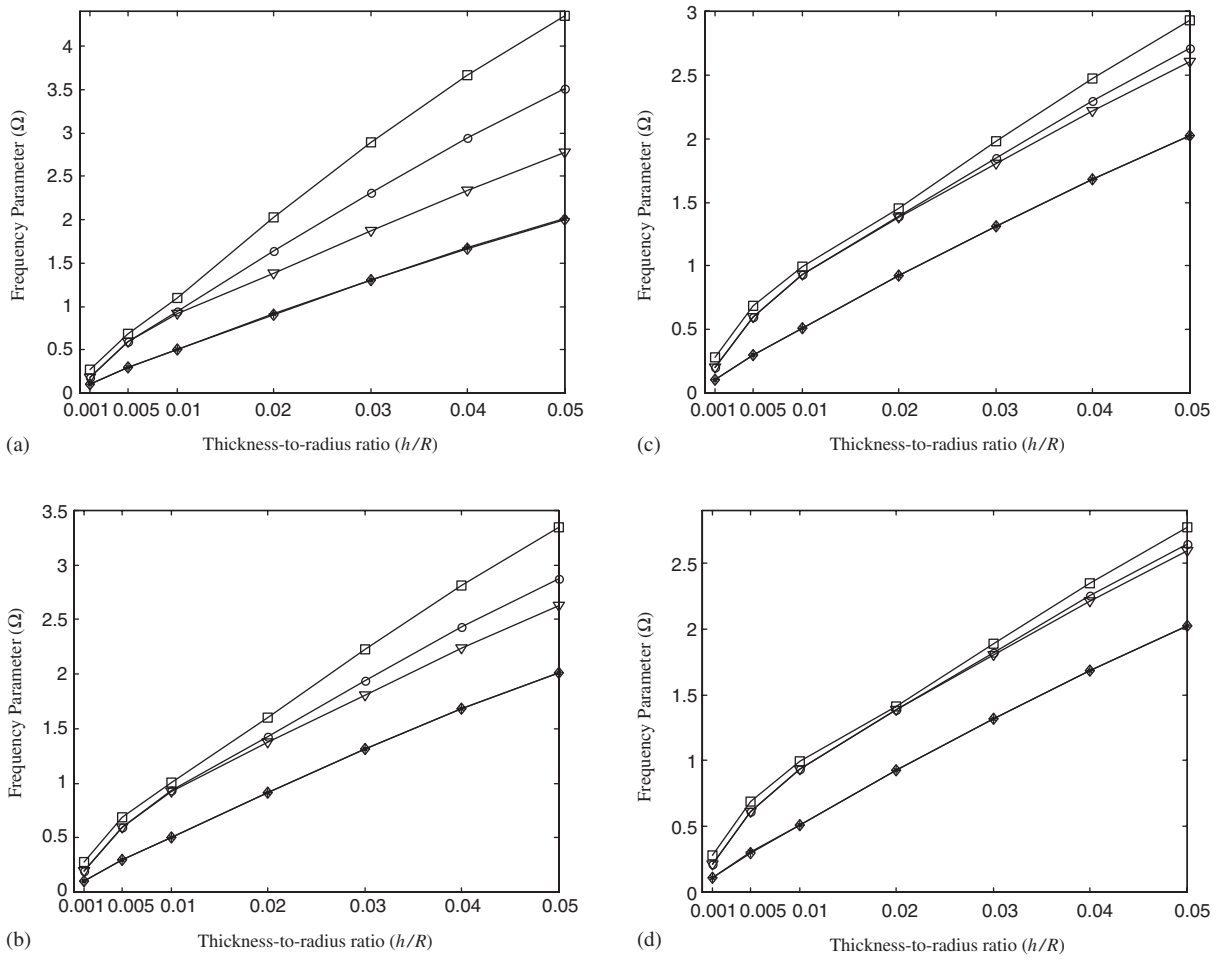

Fig. 6. Frequency parameter (Ω) versus thickness-to-radius ratio (h/R) for shells with skew angle $\alpha = 45^\circ$ and $L/R = 0.5$: diamond, mode 1; star, mode 2; triangle, mode 3; circle, mode 4; square, mode 5. (a) Subtended angle $\theta_0 = 30^\circ$; (b) $\theta_0 = 45^\circ$; (c) $\theta_0 = 60^\circ$ and (d) $\theta_0 = 75^\circ$.

mode (or wave) numbers. Therefore, one is left with the identification of the mode numbers through physical observation of the deformed surface.

Shown in Fig. 8 are the corresponding mode shapes of the skewed panel with ($\alpha = 45^\circ$) and remaining parameters are identical to those of the rectangular panel. The skewed panel exhibit symmetry and antisymmetry in the mode shapes about the skewed axes, but the amplitudes of vibration are unequal on the two parallel edges.

7. Concluding remarks

Free vibration of skewed circular open cylindrical shell has been investigated in this paper using a numerical method that is slightly a modified form of the Rayleigh–Ritz method. In the present

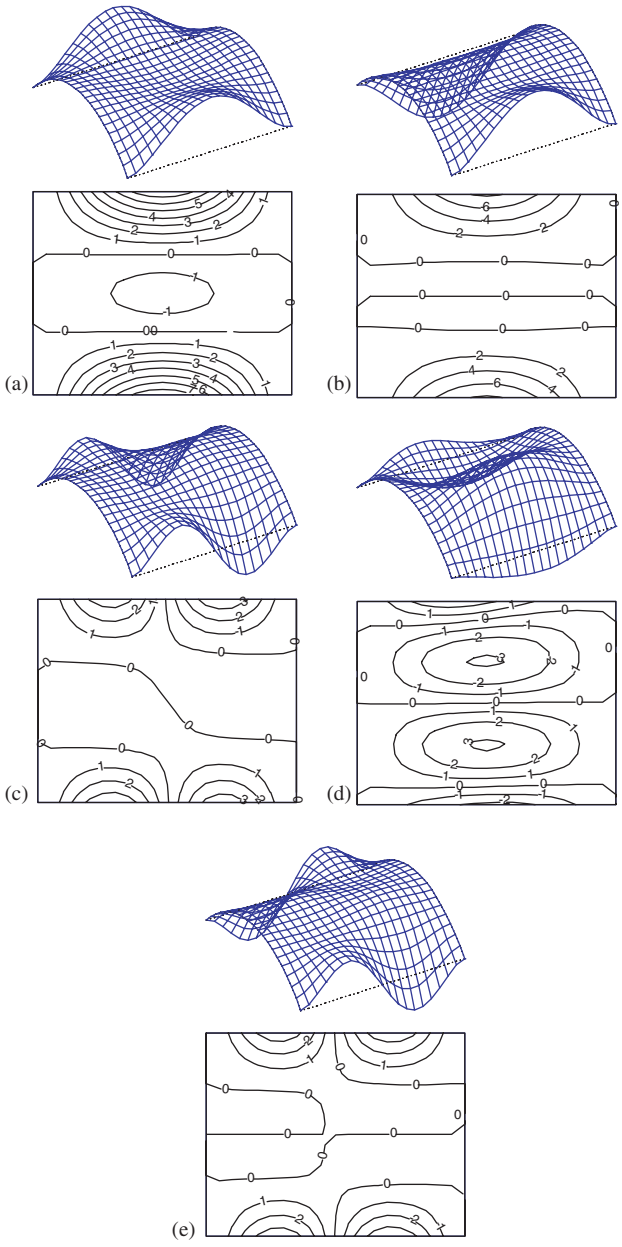

Fig. 7. First five modes of vibration of an open cylindrical shell fixed at the curved edges with skew angle $\alpha = 0^\circ$, subtended angle $\theta_0 = 60^\circ$, $h/R = 0.01$ and $L/R = 1.0$: (a) mode 1 ($\Omega = 0.14239$); (b) mode 2 ($\Omega = 0.15335$); (c) mode 3 ($\Omega = 0.30454$); (d) mode 4 ($\Omega = 0.30506$) and (e) mode 5 ($\Omega = 0.30850$).

case, the field functions are attached to the displacement and rotation components at a nodal point, whereas in the Rayleigh–Ritz method, the functions are attached to the boundary conditions. The geometry is first defined by a set of bilinear interpolating functions in natural

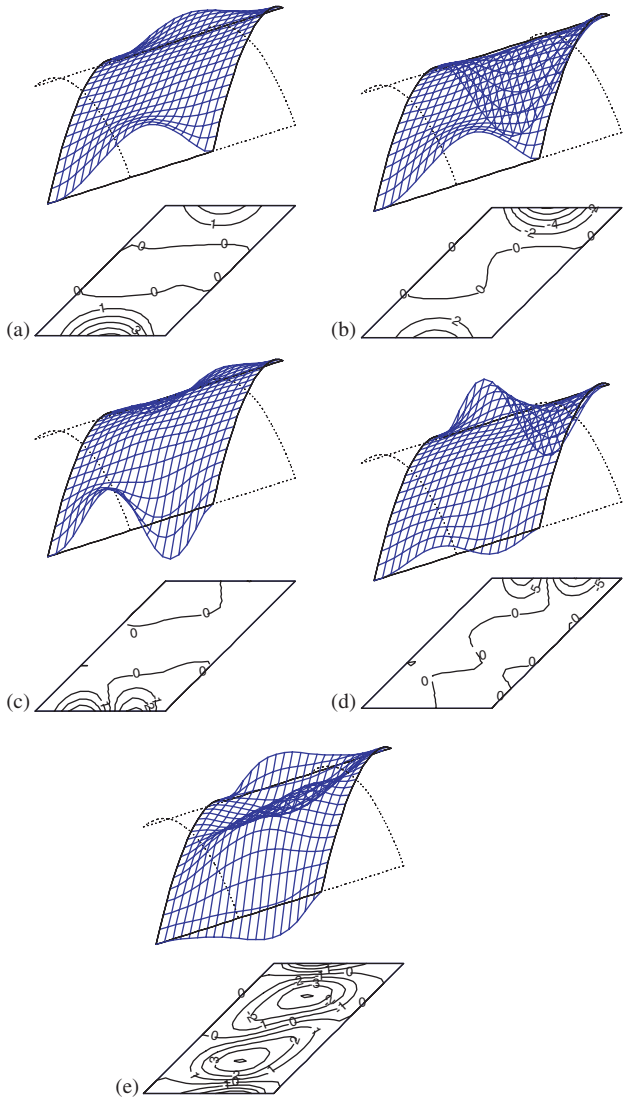

Fig. 8. First five modes of vibration of an open cylindrical shell fixed at the curved edges with skew angle $\alpha = 45^\circ$, subtended angle $\theta_0 = 60^\circ$, $h/R = 0.01$ and $L/R = 1.0$. (a) mode 1 ($\Omega = 0.18092$); (b) mode 2 ($\Omega = 0.18080$); (c) mode 3 ($\Omega = 0.34880$); (d) mode 4 ($\Omega = 0.34922$) and (e) mode 5 ($\Omega = 0.44945$).

coordinates and the displacement fields are prescribed by relatively very high-order polynomials for each dof of the pre-defined displacement nodes. Numerical results are obtained for cylindrical panels with skew angles 0–45° and subtended angles 30–75° covering a wide range from shallow-to-deep shells. As expected, the frequencies increase with the thickness and also with the skew angles. Results for the deep skew shells with opening angles 60° and 75° show that the first two modes are bunched together and the other three higher modes appear in a cluster for each case. The rectangular shell shows symmetry and antisymmetry in both the wave form and the

amplitude of vibration. On the other hand, the mode shapes of the skewed shell show similar pattern in wave form but not in the amplitude of vibration.

References

[1] A.W. Leissa, *Vibration of Shells*, NASA SP – 288, Government Printing Office, Washington, DC, 1973.
[2] M.S. Qatu, Recent research advances in the dynamic behavior of shells: 1989–2000, Part 1: laminated composite shells, *Applied Mechanics Reviews* 55 (2002) 325–350.
[3] M.S. Qatu, Recent research advances in the dynamic behavior of shells: 1989–2000, Part 2: homogeneous shells, *Applied Mechanics Reviews* 55 (2002) 415–434.
[4] A. Selmane, A.A. Lakis, Dynamic analysis of anisotropic open cylindrical shells, *Computers and Structures* 62 (1997) 1–12.
[5] N.S. Bardell, J.M. Dunsdon, R.S. Langley, On the free vibration of completely free, open, cylindrically curved, isotropic shell panels, *Journal of Sound and Vibration* 207 (1997) 647–669.
[6] N.S. Bardell, J.M. Dunsdon, R.S. Langley, Free vibration of thin, isotropic, open conical panels, *Journal of Sound and Vibration* 217 (1998) 297–320.
[7] A.V. Singh, Free vibration analysis of deep doubly curved sandwich panels, *Computers and Structures* 73 (1999) 385–394.
[8] A.V. Singh, L. Shen, Free vibration of open circular cylindrical composite shells with point supports, *ASCE Journal of Aerospace Engineering* 18 (2005) 120–128.
[9] S. Timoshenko, S. Woinowsky-Krieger, *Theory of Plates and Shells*, McGraw-Hill, New York, NY, 1959.
[10] S. Timoshenko, J.N. Goodier, *Theory of Elasticity*, third ed., McGraw-Hill, New York, NY, 1970.
[11] A.S. Saada, *Elasticity: Theory and Applications*, Krieger Publishing Company, Florida, FL, 1993.
[12] R.D. Mindlin, Influence of rotary inertia and shear on flexural motion of isotropic, elastic plates, *Journal of Applied Mechanics* 18 (1951) 31–38.
[13] P.M. Naghdi, On the theory of thin elastic shells, *Quarterly Journal of Applied Mathematics* 14 (1956) 369–390.
[14] W. Weaver Jr., P.R. Johnston, *Finite Elements for Structural Analysis*, Prentice-Hall, Englewood Cliffs NJ, 1984.
[15] A.V. Singh, T. Muhammad, Free in-plane vibration of isotropic non-rectangular plates, *Journal of Sound and Vibration* 273 (2004) 219–231.
[16] L. Librescu, *Elastostatics and Kinetics of Anisotropic and Heterogeneous Shell Type Structures*, Noordhoff International Publishing, Leyden, The Netherlands, 1975.
[17] S. Kandasamy, A Variational Approach for the Free and Forced Vibrations of Open Cylindrical shells, Master's Thesis, The University of Western Ontario, London, Canada, 2004.